

will be affected. As a result, also the interaction terms with potential migrating groups will be altered.

Recently, a similar theory of catalytic activity has been worked out.<sup>11</sup>

## References and Notes

- (1) (a) R. B. Woodward and R. Hoffmann, *J. Am. Chem. Soc.*, **87**, 395 (1965); (b) *ibid.*, **87**, 2046 (1965); (c) *ibid.*, **87**, 2511 (1965).
- (2) A. G. Anastassiou, *Chem. Commun.*, 15 (1968).
- (3) (a) J. A. Berson and G. L. Nelson, *J. Am. Chem. Soc.*, **92**, 1096 (1970); (b) J. A. Berson and L. Salem, *ibid.*, **94**, 8917 (1972).
- (4) O. Eistenstein, J.-M. Lefour, and N. T. Anh, *Chem. Commun.*, 969 (1971).
- (5) K. Fukui, *Acc. Chem. Res.*, **4**, 57 (1971).
- (6) G. A. Shchembelov and Yu. Ustynyuk, *Theor. Chim. Acta*, **24**, 389 (1972).
- (7) J. R. de Dobbelaere, J. W. de Haan, H. M. Buck, and G. J. Visser, *Theor. Chim. Acta*, **31**, 95 (1973).
- (8) J. R. de Dobbelaere, E. L. van Zeeventer, J. W. de Haan, and H. M. Buck, *Theor. Chim. Acta*, **38**, 241 (1975).
- (9) R. C. Bingham and M. J. S. Dewar, *J. Am. Chem. Soc.*, **94**, 9107 (1972).
- (10) (a) G. R. Krow and J. Reilly, *J. Am. Chem. Soc.*, **97**, 3837 (1975); (b) see R. K. Lustgarten and H. G. Richey, Jr., *ibid.*, **96**, 6393 (1974), and ref 54-56.
- (11) A. Imamura and T. Hirano, *J. Am. Chem. Soc.*, **97**, 4192 (1975).
- (12) The experimental and theoretical activation enthalpies are in good agreement. See ref 8.
- (13) The geometry of the cyclopentadiene transition state has been optimized with respect to eight variables (see Table II). A fully optimized transition state as calculated by Ustynyuk et al. shows no essential difference.<sup>6</sup> Our optimization resulted in an approximately symmetric structure as can be derived from Table II, which shows  $\beta$  approximately equal to  $\gamma$  and  $\delta = \epsilon$ . Consequently for all other cyclic systems the symmetry plane was assumed, while optimizing all other variables. In all systems it was assumed that the transition state has only one negative force constant.
- (14) The reason for the cyclic symmetry properties in the present case is probably to be ascribed to the enhanced flexibility of the system. This enables a closer approach between migration origin and terminus in the transition state as compared to cycloheptatriene. In the acyclic pentadienyl system therefore the  $p_z$  orbitals of migration origin and terminus overlap in order to form a partial  $\pi$  bond. In the cycloheptatriene system, the two carbon atoms involved are held apart by the rather rigid ethylene moiety.
- (15) NOTE ADDED IN PROOF. In reality the  $H_{1s}$  level lies about  $1\beta$  ( $\beta = -2.4$  eV) below the zero level, but this does not affect any of the conclusions.

## Global Topology of Triatomic Potential Surfaces

Ernest R. Davidson

Contribution from the Chemistry Department, University of Washington, Seattle, Washington 98195. Received July 26, 1976

**Abstract:** A new coordinate system for describing triatomic molecules is introduced. Within this coordinate system various topological features of importance are discussed. Particular emphasis is placed on the Jahn-Teller theorem and the resulting branch-cuts on the potential surface.

Potential surfaces are of importance in chemistry for explaining geometry, spectra, and chemical reactions. Triatomic potential surfaces (especially for excited states) have recently become of even greater interest because of work in plasmas, lasers, and atmospheric pollution associated with various aspects of the energy crisis. Unlike diatomic molecules which are fairly well characterized, polyatomic potential surfaces are only vaguely understood. While the general features expected for a diatomic molecule potential curve over the whole range of possible molecular conformations are well known, such a global topology for triatomic molecules is not usually discussed.

### General Considerations

A potential surface, for the purpose of the present discussion, will be a function  $U(X_1, \dots, X_K)$  generated as one of the solutions to an electronic (Born-Oppenheimer) Schrödinger equation

$$H\psi(r_1 \dots r_N; X_1 \dots X_K) = U(X_1 \dots X_K)\psi(r_1 \dots r_N; X_1 \dots X_K) \quad (1)$$

where the  $r_i$  are electronic coordinates and the  $X_j$  are coordinates for describing the conformation of the nuclei in the molecule. The operator  $H$  in the simplest approximation is just the usual electronic hamiltonian involving electronic kinetic energy and coulomb interactions,

$$H = -\frac{\hbar^2}{2m} \sum_i \nabla_i^2 - e^2 \sum_{i \neq A} \sum_A Z_A r_{iA}^{-1} + e^2 \sum_{A \neq B} Z_A Z_B r_{AB}^{-1} + e^2 \sum_{i \neq j} r_{ij}^{-1} \quad (2)$$

For discussing a potential surface  $U$  it is sufficient to pick the complete set of coordinates  $X_i$  which affect the shape or size

of the molecule but not its position or orientation in space. Hence for three or more atoms  $K$  is  $3N_A - 6$  where  $N_A$  is the number of atoms (for a global discussion of  $U$  the question of whether the molecule is "linear" or not does not enter).

The Schrödinger equation for a molecule actually defines an infinite family of potential surfaces, of course. Because of the possibility of intersections, great care must be exercised in identifying a surface. In general, there are certain elements of symmetry such as electron spin which are global in nature (i.e., commute with  $H$  for all values of the  $X_i$ ). Diatomic molecules are always linear and triatomics are always planar, while larger polyatomics have no global geometric symmetry. In any case, the electronic wave functions and associated potential surfaces can be labeled with whatever global symmetry is present. Beyond that, at each set of nuclear coordinates  $X_i$  the potential surfaces of the same global symmetry are simply numbered in order of increasing energy. With this convention the  $k$ th potential energy surface of symmetry  $\Gamma$ ,  $U_k(\Gamma)$ , will be a continuous function of the  $X_i$ . For diatomic molecules this convention is known to lead to smooth (differentiable) functions  $U_k$  (except for the  $2s\sigma_g$  and  $3d\sigma_g$  curves<sup>1</sup> for  $H_2^+$ ) which do not intersect other curves of the same symmetry<sup>2</sup> in the open interval  $0 < R < \infty$ .

By global topology is meant the study of the shape and structure of the potential energy surface over the entire range of the nuclear position coordinates. Certain kinds of structural features are well-known. For example, wherever two nuclei coincide the potential surface has a coulomb singularity. This singularity is easily removed by subtracting the nuclear-nuclear repulsion from  $U$  to get the "electronic energy"  $U_c$

$$U_c = U - e^2 \sum_{A \neq B} Z_A Z_B r_{AB}^{-1} \quad (3)$$

Near  $r_{AB} = 0$ ,  $U_e$  continuously approaches the united atom limit equivalent to replacing nuclei A and B by one nucleus of charge  $Z_A + Z_B$ . If both nuclei have atomic numbers greater than two, however, the wave function and  $U_e$  will change rapidly over a very small range of  $R_{AB}$  as the inner electron cores penetrate each other.

There will also be asymptotic regions corresponding to fragmenting the molecule into various pieces. In the limit of large separation between the fragments,  $U$  will be independent of the exact separation or orientation of the fragments and will be just the sum of appropriate  $U$ 's for each individual fragment.

Of great interest to chemists has been the structure of the first and second derivatives of  $U$  with respect to nuclear coordinates. At most points on the surface one can define the gradient vector with elements  $\partial U/\partial X_i$  and the force constant matrix with elements  $\partial^2 U/\partial X_i \partial X_j$ . Further, one can diagonalize the force constant matrix at each point to obtain local normal coordinates and local canonical second derivatives.

The point where the gradient vanishes and all second derivatives are positive is a stable local minimum which may correspond to the geometry of a possible isomer formed from the atoms present. Assumptions concerning atomic radii additivity<sup>3</sup> to give bond lengths and Walsh's rules<sup>4,5</sup> to give bond angles (plus the observation that the most electronegative atoms appear in terminal positions) often allow intelligent prediction of the location of minima in  $U$ .

The gradient may also vanish at a point where one canonical second derivative is negative. In this case the point is a transition state in an isomeric rearrangement (in a global sense which includes exchange reactions as isomerizations). At this point the normal coordinate associated with the negative second derivative is the local reaction coordinate. In practice transition states are not as well understood as minima (because they are not as directly deduced from experiments) and are much harder to locate in a multidimensional space.<sup>6</sup> The gradient may also vanish at points with more than one negative second derivative. These more general saddle points have not yet been invoked in explaining reactions since there is usually a lower energy pathway for the reactions.<sup>7</sup> Because of the importance of the signs of the canonical second derivatives, a map showing the locus of inflection points where one (or more) second derivative is zero would be of interest. These surfaces would divide the space into regions of differing numbers of negative second derivatives.

Finally, an essential feature of most  $K$  dimensional potential surfaces for molecules with three or more atoms is a  $K - 2$  dimensional network of branch-cuts along which  $U$  (and the electronic wave function) is not differentiable with respect to the nuclear coordinates.<sup>8</sup> Any motion of the nuclei during vibrations, reactions, or collisions which brings the nuclear conformation near such a cut must be treated cautiously since the adiabatic approximation is certainly not valid and a coupled-state diabatic treatment must usually be introduced to obtain correct understanding of the experimental results.<sup>9</sup>

As was shown by Teller,<sup>8</sup> these branch-cuts arise whenever two potential surfaces of the same global symmetry are degenerate. Unlike diatomic molecules, such "crossings" are allowed for polyatomic molecules. At certain special values of the nuclear coordinates, the electronic hamiltonian may commute with additional point-group operators so that the "local" symmetry at the "site"  $X_1, X_2, \dots, X_k$  may be higher than the global symmetry. At such a site the wave function must transform like an irreducible representation of the local symmetry group. The most easily understood degeneracies for polyatomic molecules are those which occur at sites of very high symmetry and which are required by symmetry (as in the Jahn-Teller theorem<sup>10</sup>). The next most easily understood degeneracies are those (as in  $\text{NO}_2$ ) which occur at sites of

higher than global symmetry between states of the same global symmetry but different local symmetry.<sup>11</sup> In this case the intersection is allowed, but not required, by symmetry. As shown by Longuet-Higgins, model hamiltonians (and presumably real molecules) can also be found for which degeneracies occur at the lowest symmetry points.<sup>12</sup>

To see the essential features of such a point of degeneracy consider two surfaces of the same global symmetry, say  $U_1$  and  $U_2$ , which are degenerate at a point  $(X_1^0, \dots, X_k^0)$  and have wave functions  $\psi_1^0$  and  $\psi_2^0$  at that point. Then near  $X^0$  energy can be computed by first-order degenerate perturbation theory. That is,  $H$  can be expanded at  $X^0 + \delta$  as

$$H = H^0 + \sum_j (\partial H/\partial X_j)_0 \delta_j \quad (4)$$

and the first-order approximation to the energies  $U_1$  and  $U_2$  can be formed by diagonalizing the  $2 \times 2$  matrix with elements

$$H_{pq} = \langle \psi_p^0 | H | \psi_q^0 \rangle \quad (5)$$

$p, q = 1 \text{ or } 2$

Substitution gives

$$H_{pq} = \delta_{pq} U^0 + \sum_j \langle \psi_p^0 | (\partial H/\partial X_j)_0 | \psi_q^0 \rangle \delta_j \quad (6)$$

Not let  $\xi_k$  ( $k = 1, 2, 3$ ) be vectors with components

$$\xi_{j1} = \frac{1}{2} [\langle \psi_1^0 | (\partial H/\partial X_j)_0 | \psi_1^0 \rangle + \langle \psi_2^0 | (\partial H/\partial X_j)_0 | \psi_2^0 \rangle] \quad (7)$$

$$\xi_{j2} = \frac{1}{2} [\langle \psi_1^0 | (\partial H/\partial X_j)_0 | \psi_1^0 \rangle - \langle \psi_2^0 | (\partial H/\partial X_j)_0 | \psi_2^0 \rangle] \quad (8)$$

$$\xi_{j3} = \langle \psi_1^0 | (\partial H/\partial X_j)_0 | \psi_2^0 \rangle \quad (9)$$

Then the potential surfaces very near  $X^0$  can be seen to be

$$U = U^0 + \xi_1 \cdot \delta \pm [(\xi_2 \cdot \delta)^2 + (\xi_3 \cdot \delta)^2]^{1/2} \quad (10)$$

Thus  $U$  is independent of displacements  $\delta$  orthogonal to the  $\xi_k$  (at least  $K - 3$  directions). Further, for a displacement  $\delta$  orthogonal to  $\xi_2$  and  $\xi_3$ ,  $U_1$  and  $U_2$  remain degenerate. That is, the intersection of  $U_1$  and  $U_2$  is only a  $K - 2$  dimensional region around  $X^0$  unless  $\xi_2$  and  $\xi_3$  happen to be linearly dependent or one of them vanishes (which will usually not happen if  $\Psi_1$  and  $\Psi_2$  are of the same global symmetry<sup>13</sup>).

If  $\bar{U}$  is defined as  $\frac{1}{2}(U_1 + U_2)$ , then  $U_1 - \bar{U}$  and  $U_2 - \bar{U}$  depend only on  $\xi_2 \cdot \delta$  and  $\xi_3 \cdot \delta$ . As shown in Figure 1, a graph of these functions gives the upper and lower portions of a right circular cone with vertex at the origin. This is the typical Teller splitting<sup>8</sup> which is linear in the norm of the displacement vector  $\delta$ .

The electronic wave functions also have some peculiar properties near this intersection. If

$$\cos \alpha = (\xi_2 \cdot \delta)/A \quad (11)$$

$$\sin \alpha = (\xi_3 \cdot \delta)/A \quad (12)$$

and

$$A = [(\xi_2 \cdot \delta)^2 + (\xi_3 \cdot \delta)^2]^{1/2} \quad (13)$$

then

$$U - \bar{U} = \pm A \quad (14)$$

$$\psi_2 = \cos(\alpha/2)\psi_1^0 + \sin(\alpha/2)\psi_2^0 \quad (15)$$

and

$$\psi_1 = -\sin(\alpha/2)\psi_1^0 + \cos(\alpha/2)\psi_2^0 \quad (16)$$

Thus if the projection of  $\delta$  onto the  $\xi_2, \xi_3$  plane is moved once around a closed curve encircling the origin,  $\alpha$  will change by



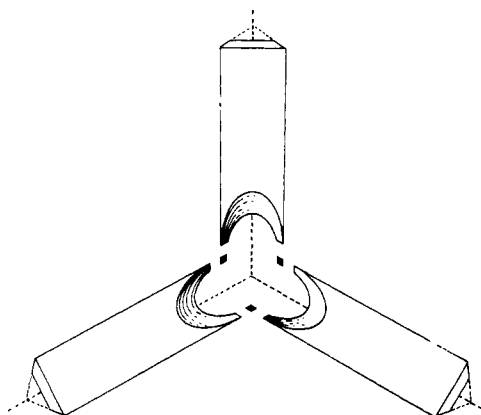


Figure 5. Constant energy contours for the  ${}^2A'$  ground state of  $H_3$ . Each saddle point of the exchange reaction is marked by a solid square.

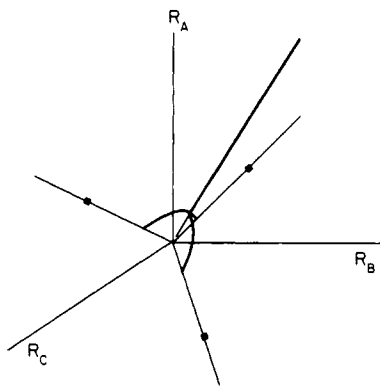


Figure 6. Branch lines for the lowest  ${}^2A'$  state of  $H_3$ . For reference, each saddle point is marked by a solid square and the loci of symmetrical linear molecules are shown.

to three hydrogen atoms with energy about 6 kcal/mol above the minimum possible potential energy. The wide flat shape in the asymptotic region arises from the rather small range of stretching motion possible accompanied by almost complete freedom to rotate the  $H_2$  molecule relative to the H atom (i.e., all points in the surface  $R_A + R_B = R_{AB} = \text{constant}$ , for  $R_C$  large, are accessible). It is known that the linear shape is lower in energy at closer distances of approach.<sup>14</sup> This is reflected in the sketch by the contours extending to closer approach distances for linear than for nonlinear conformations. The known saddle points are indicated by solid squares on the figure. Detailed information such as the shape of surfaces of inflection are not yet available even for this very simple system.

Figure 6 shows a sketch of the branch-cut network for  $H_3$ . For reasonable values of the coordinates it is known that the only degeneracy expected occurs at  $D_{3h}$  conformations where simple molecular orbital theory predicts a  ${}^2E'$  ground state. At very small distances, however, the wave function must approach the united atom  $1s^22s\ ^2S$  (lithium) limit. Hence, along the line of  $D_{3h}$  conformations the  ${}^2E'$  state must intersect a  ${}^2A_1'$  state which has the same global ( ${}^2A'$ ) symmetry as each component of  ${}^2E'$ . At small  $C_{2v}$  distortions from  $D_{3h}$ , the  ${}^2E'$  state splits into  ${}^2A_1$  and  ${}^2B_2$  while  ${}^2A_1'$  gives only  ${}^2A_1$ . At very large  $C_{2v}$  distortions, say linear symmetric,  ${}^2B_2$  correlates with the known  ${}^2\Sigma_u^+$  wave function of the saddle point region while  ${}^2A_1$  would become  ${}^2\Sigma_g^+$ . Thus at each bond angle between 60 and 180° for a  $C_{2v}$  conformation one would expect the wave function to be  ${}^2B_2$  at reasonable bond lengths but  ${}^2A_1$  at very short bond lengths. For angles much less than 60° the wave function would be expected to be  ${}^2A_1$  at both large and small bond lengths and can change continuously from one form to

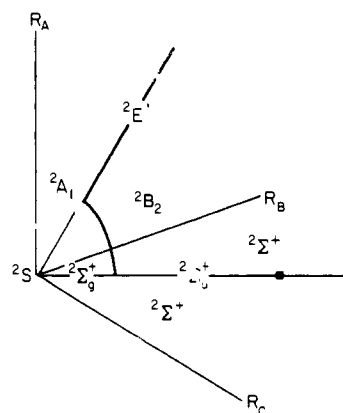


Figure 7. Symmetry labels of the wave function for branch lines of the lowest  ${}^2A'$  state of  $H_3$  in one  $C_{2v}$  plane and one linear plane. The saddle point is marked by a solid square and the symmetrical linear locus formed by the intersection of the  $C_{2v}$  and linear planes is shown.

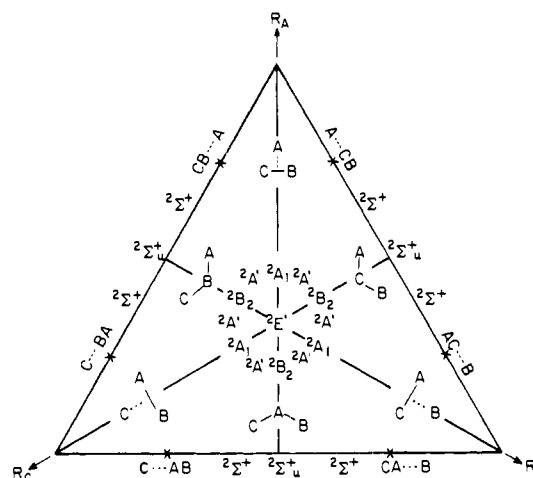


Figure 8. Structure of the lowest  ${}^2A'$  state of  $H_3$  in a plane perpendicular to the equal bond length ( $D_{3h}$ ) direction. Relative minima are marked by X.

the other. Figure 6 is the simplest diagram consistent with these facts. Figure 7 summarizes the symmetry changes on one  $C_{2v}$  plane and one linear plane caused by this branch-cut.

It should perhaps be emphasized again that it is always possible to pass continuously from one of these wave functions to another by following a path which avoids the branch-cut. Although a calculation at  $D_{\infty h}$  conformations might have treated  ${}^2\Sigma_g^+$  and  ${}^2\Sigma_u^+$  as two states which cross, in a global sense the lower of them at each point is part of the same  ${}^2\Sigma^+$   $C_{\infty v}$  surface. Similarly the  ${}^2A_1$  and  ${}^2B_2$  surfaces might have been thought to be two states in a  $C_{2v}$  restricted calculation of the energy but the lower of them at each point is in reality part of the same  ${}^2A'$  potential surface.

Figure 8 emphasizes this continuous passage between states of different symmetry in a plane perpendicular to the  $D_{3h}$  direction. Because there are three different  $C_{2v}$  subgroups of  $D_{3h}$ , three different sets of  ${}^2A_1$ ,  ${}^2B_2$  pairs of labels are encountered which are equivalent but differ in which  $\sigma_v$  mirror plane from  $D_{3h}$  is preserved. The minimum energy for  $H_3$  in this plane is marked by X. It is interesting that this minimum occurs at a point of low symmetry and hence there are six equivalent minima separated by barriers for exchange and rotation. Within this plane, the potential surface is an example of the usual Jahn-Teller distortion<sup>10</sup> (an intrinsically degenerate pair of distortion coordinates and an intrinsically degenerate potential surface) and has been discussed as such by Porter et al.<sup>15</sup>

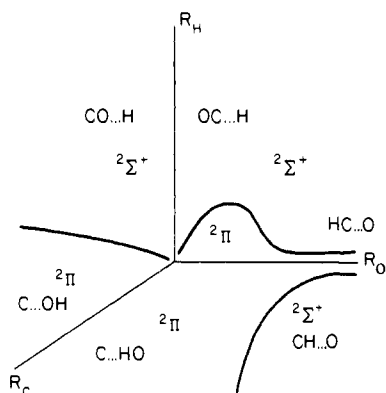


Figure 9. Branch lines for the lowest  $2A'$  state of HCO.

Longuet-Higgins<sup>12</sup> uses an example like the  $D_{3h}$   $2E'$  branch-cut of  $H_3$  and this plane perpendicular to the  $D_{3h}$  direction as an example of a sign changing loop. Any loop in this plane encircling the  $D_{3h}$  line (center of the triangle) will give a change in sign of the wave function. Figure 6 introduces an additional kind of point not considered by Longuet-Higgins. A loop encircling two legs of the branch-cut can easily be shown to involve no sign change even in the limit that the loop shrinks to a small circle around the point where the branch-cuts join together. For a branch-cut which terminates in a plane of linear conformations, it is still true that a loop in that plane around the terminus will give a sign change.

**(B) Other Triatomic Systems.** Even less is known about the global properties of potential surfaces for other triatomic molecules. Figure 9 shows the branch-cuts resulting from an extended Hückel calculation for the lowest  $2A'$  state of HCO (plus consideration of various possible limits). In this case the branch-cuts seem to run entirely through various linear conformations. If other branches are present they have not yet been discovered. Other cuts are almost certain to be present very near the united atom. The switch from  $2\Sigma^+$  to the  $2A'$  component of  $2\Pi$  along the  $OC \cdots H$  approach has been previously recognized as an important part of the reason that OCH is a nonlinear molecule.<sup>16</sup> The switch from  $2\Pi$  to  $2\Sigma$  near the  $R_O$  axis is associated with the switch from the  $4S$  ground state of the N atom to the  $2\Pi$  ground state of CH.

For this example, there would seem to be no loops which can be drawn around the branch-cut. This brings up a problem in interpretation. For a linear triatomic molecule there are usually said to be four rather than three coordinates because one of the rotational coordinates of the nonlinear molecule becomes an internal coordinate. There would seem to be no way to do this consistently on a global scale short of always including all three rotational degrees of freedom and treating the surface in six dimensions. For the six-dimensional treatment, the global symmetry would be only  $C_1 \otimes O_3$  although every point has at least  $C_s \otimes O_3$  site symmetry. Branch-cuts would then be four dimensional (as for example the  $2\Pi$  degenerate pair of states in a full Renner-Teller treatment<sup>17</sup>). As shown by Longuet-Higgins,<sup>12</sup> simultaneous intersection of three surfaces would normally be zero dimensional, but for the special case of  $\Sigma$ - $\Pi$  intersection in triatomic molecules two of the splitting directions become linearly dependent and two have no effect on the energy so the triple intersection is three dimensional. No theorems concerning sign reversals caused by mixing of three states under distortions in the splitting directions have been given. For this special case it is clear that two fixed wave functions for the  $2\Pi$  state can be combined into a  $2A'$  and  $2A''$  pair relative to the molecular plane defined by the distorted molecule and then the  $2A'$  function thus formed mixes with the  $2\Sigma^+$  wave function. The relevant distortion coordinates are the two perpendicular bends and one stretching mode.

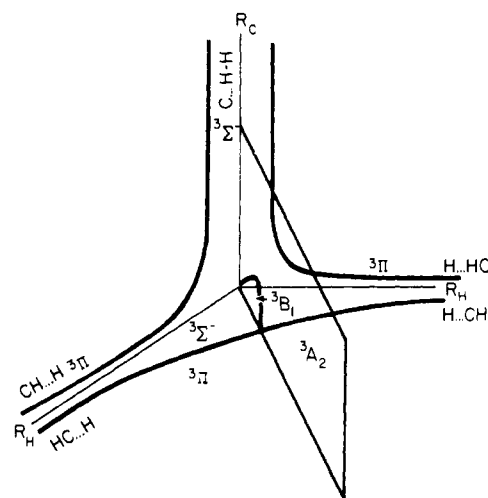


Figure 10. Branch lines for the lowest  $3A''$  state of  $CH_2$ . The  $C_{2v}$  plane is outlined for reference.

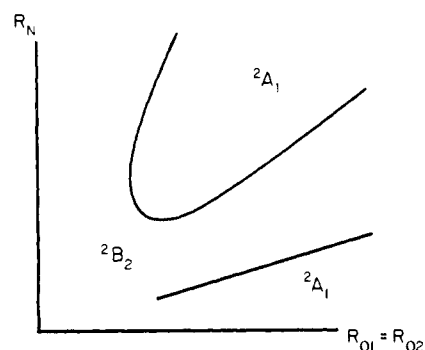


Figure 11. Branch lines for the lowest  $2A'$  state of  $NO_2$  in the  $C_{2v}$  plane.

Figure 10 shows the branch-cuts for  $CH_2$  computed in conjunction with C. F. Bender of Lawrence Livermore Laboratory. Even with fairly elaborate SCF-CI methods it is difficult to determine the positions of the branch-cuts accurately because SCF-CI methods do not give reliable results at unusual bond lengths. The diagram agrees with qualitative expectations, however, that CH should be  $2\Pi$  at most bond lengths but  $4\Sigma^-$  near the united atom limit. Also  $CH_2$  at  $C_{2v}$  configurations is known to be  $3B_1$  at obtuse bond angles but clearly should be  $3A_2$  for very acute bond angles. The equilibrium geometry for  $CH_2$  lies near the center of the  $3B_1$  region. This would be a very interesting example for study of the exchange reactions  $C + H_2 \rightarrow CH + H$  or  $HC + H \rightarrow H + CH$  because of the expected difficulties caused by the branch-cuts. The complexity of the branching diagram for  $CH_2$  and similar "simple" molecules also makes clear the difficulty in obtaining an approximate function to represent the potential surface over a wide range of coordinates.

As a final example, Figure 11 presents a part of the branching diagram for  $NO_2$  in the  $C_{2v}$  plane. This example is interesting because the  $2B_2$  and  $2A_1$  regions each contain a minimum in the  $C_{2v}$  plane. These were originally treated as two states rather than two parts of the lowest  $2A'$  state of  $NO_2$ . Detailed calculations<sup>11</sup> have indicated that when more general conformations are considered, the  $2B_2$  "minimum" is actually a saddle point from which one can pass by a down-hill path to the  $2A_1$  minimum (through non- $C_{2v}$  conformations). This is a quite complicated example and only a small part of the potential surface has been accurately studied.

## Conclusion

Some tentative examples have been presented to illustrate the need for global understanding of the potential surface. Although the Teller theorem is well-known, its implications have not been carefully considered previously. The network of branch-cuts is a topological feature which must be carefully considered in a global discussion of polyatomic potential surfaces because the existence of such a network to a certain extent invalidates the adiabatic approximation for describing nuclear motion. Because of the possibility of sign-reversing loops which lie at a great distance from branch-cut singularities, it is generally impossible to assign an electronic wave function to each nuclear configuration in such a way that the wave function is continuous in nuclear coordinates.

**Acknowledgment.** The author is grateful to Charles F. Bender and Lawrence Livermore Laboratory for calculations on  $\text{CH}_2$ . This research was supported by the National Science Foundation.

## References and Notes

- (1) D. R. Bates, K. Ledsham, and A. L. Stewart, *Phil. Trans. R. Soc. London, Ser. A*, **246**, 215 (1953).
- (2) F. Hund, *Z. Phys.*, **40**, 742 (1927).
- (3) J. C. Slater, *J. Chem. Phys.*, **41**, 3199 (1964).
- (4) A. D. Walsh, *J. Chem. Soc.*, 2260 (1953).
- (5) R. J. Buenker and S. D. Peyerimhoff, *Chem. Rev.*, **74**, 127 (1974).
- (6) J. N. Murrell and K. J. Laidler, *Trans. Faraday Soc.*, **64**, 371 (1968).
- (7) J. N. Murrell and G. L. Pratt, *Trans. Faraday Soc.*, **66**, 1680 (1970).
- (8) E. Teller, *J. Phys. Chem.*, **41**, 109 (1937).
- (9) E. E. Nikitin, *Adv. Chem. Phys.*, **28**, 317 (1975), and references therein.
- (10) H. A. Jahn and E. Teller, *Proc. R. Soc. London, Ser. A*, **161**, 220 (1937).
- (11) C. F. Jackels and E. R. Davidson, *J. Chem. Phys.*, **64**, 2908 (1976).
- (12) H. C. Longuet-Higgins, *Proc. R. Soc. London, Ser. A*, **344**, 147 (1975).
- (13) K. R. Naqvi and W. B. Brown, *Int. J. Quantum Chem.*, **6**, 271 (1972); K. R. Naqvi, *Chem. Phys. Lett.*, **15**, 634 (1972); G. J. Hoytink, *ibid.*, **34**, 414 (1975), have recently criticized this proof as well as the simpler dimensionality proof of J. V. Neumann and E. P. Wigner, *Z. Phys.*, **30**, 467 (1929), and the examples given by G. H. Herzberg and H. C. Longuet-Higgins, *Discuss. Faraday Soc.*, **No. 35**, 77 (1963). As pointed out by Longuet-Higgins in ref 12, these criticisms are invalid because they miss the point of the original proofs. The phrase "usually not happen" in the text refers to the fact that the family of hamiltonians for which  $\xi_2$  and  $\xi_3$  are linearly dependent is a set of measure zero in the family of all hamiltonians which can be constructed.
- (14) B. Liu, *J. Chem. Phys.*, **58**, 1925 (1973).
- (15) R. N. Porter, R. M. Stevens, and M. Karplus, *J. Chem. Phys.*, **49**, 5163 (1968).
- (16) J. W. C. Johns, S. H. Priddle, and D. A. Ramsey, *Discuss. Faraday Soc.*, **No. 35**, 90 (1963).
- (17) R. Renner, *Z. Phys.*, **92**, 172 (1934).

# Synthesis, Structure, and Bonding of the Tetrameric Cyclopentadienyliron Sulfide Monocation, $[\text{Fe}_4(\eta^5\text{-C}_5\text{H}_5)_4(\mu_3\text{-S})_4]^+$ : Stereochemical Consequences Due to Oxidation of a Cubane-Like $\text{Fe}_4\text{S}_4$ Core<sup>1</sup>

Trinh-Toan, W. Peter Fehlhammer, and Lawrence F. Dahl\*<sup>2</sup>

Contribution from the Department of Chemistry, University of Wisconsin, Madison, Wisconsin 53706. Received June 16, 1976

**Abstract:** The  $[\text{Fe}_4(\eta^5\text{-C}_5\text{H}_5)_4(\mu_3\text{-S})_4]^+$  monocation was obtained from oxidation of the neutral  $\text{Fe}_4(\eta^5\text{-C}_5\text{H}_5)_4(\mu_3\text{-S})_4$  cluster by different oxidizing agents such as  $\text{AgBF}_4$ ,  $\text{I}_2$ , and  $\text{Br}_2$ . An x-ray diffraction study of the  $[\text{Fe}_4(\eta^5\text{-C}_5\text{H}_5)_4(\mu_3\text{-S})_4]\text{Br}$  salt reveals that the one-electron oxidation of the neutral species distorts the  $\text{Fe}_4\text{S}_4$  core from a tetragonal  $D_{2d}\text{-}42m$  geometry containing two electron-pair bonding and four nonbonding Fe-Fe distances of 2.64 and 3.36 Å, respectively, to an orthorhombic  $D_{2d}\text{-}222$  geometry possessing three pairs of Fe-Fe distances of 2.65, 3.19, and 3.32 Å. This preferential shortening of two of the four long Fe-Fe distances in the monocation relative to those in the parent molecule is attributed to the removal of an electron from an antibonding iron cluster orbital of degenerate  $e$  representation (under  $D_{2d}$  symmetry), which thereby produces the observed orthorhombic distortion via a first-order Jahn-Teller effect. Crystals of  $[\text{Fe}_4(\eta^5\text{-C}_5\text{H}_5)_4(\mu_3\text{-S})_4]\text{Br}$  are monoclinic with space group symmetry  $A2/a$  and lattice constants  $a = 15.668$  (2) Å,  $b = 13.289$  (2) Å,  $c = 13.996$  (2) Å,  $\beta = 124.48$  (1)°, and  $\rho_{\text{obsd}} = 1.94$  vs.  $\rho_{\text{calcd}} = 1.91$  g cm<sup>-3</sup> for  $Z = 4$ . Least-squares refinement gave  $R_1 = 8.0\%$  and  $R_2 = 7.1\%$  for 1053 independent diffractometry data with  $I \geq 2.0\sigma(I)$ .

As part of an extensive examination of the influence of valence electrons on the geometries of various classes of ligand-bridged metal clusters via oxidation and/or reduction of the neutral species, we have concentrated upon the synthesis and structural characterization of cubane-like metal clusters containing four transition metal atoms and four triply bridging ligands at the alternate apices of a distorted cube.<sup>3,4</sup>

Our preparation of the  $[\text{Fe}_4(\eta^5\text{-C}_5\text{H}_5)_4(\mu_3\text{-S})_4]^+$  monocation by oxidation of the diamagnetic neutral tetramer together with its structural determination was a consequence not only of its importance from theoretical considerations but also of its possible biological implications (during the time of its synthesis by us<sup>1</sup> and independently by Ferguson and Meyer<sup>5</sup>) in that the neutral parent<sup>6</sup> was then proposed<sup>7</sup> to be a possible model for the redox center of the reduced form of the high-potential iron protein isolated from the photosynthetic bacterium *Chromatium*.<sup>8-10</sup> The fact that this paramagnetic

$[\text{Fe}_4(\eta^5\text{-C}_5\text{H}_5)_4(\mu_4\text{-S})_4]^+$  monocation possessed a hitherto unknown molecular orbital electronic configuration for a cubane-like species made it especially desirable to determine the stereochemical effect of a one-electron oxidation on the  $\text{Fe}_4\text{S}_4$  core. The resulting structural information presented here has provided a requisite basis for our subsequent studies<sup>4</sup> directed toward a systematization of the topological nature of cubane-like transition metal clusters from which the geometries of such complexes can be correlated with the varying number of electrons in the metal cluster orbitals.

## Experimental Section

**Preparation and Properties.** (a) **General Remarks.** The neutral  $\text{Fe}_4(\eta^5\text{-C}_5\text{H}_5)_4(\mu_3\text{-S})_4$  complex was prepared as described previously.<sup>6b</sup> The cationic species was obtained in nearly quantitative yields from oxidation of  $\text{Fe}_4(\eta^5\text{-C}_5\text{H}_5)_4(\mu_3\text{-S})_4$  by different oxidizing agents such as  $\text{AgBF}_4$ ,  $\text{I}_2$ , and  $\text{Br}_2$ . The  $[\text{Fe}_4(\eta^5\text{-C}_5\text{H}_5)_4(\mu_3\text{-S})_4][\text{PF}_6]$  salt